ELSEVIER

Catalysis Today 50 (1999) 589–601

CATALYSIS TODAY

Towards understanding the mechanism for the selective hydrogenation of maleic anhydride to tetrahydrofuran over palladium

Venkataraman Pallassana[a], Matthew Neurock[a,*], George Coulston[b]

[a]*Department of Chemical Engineering, University of Virginia, Charlottesville, VA 22903, USA*
[b]*DuPont CR&D, Experimental Station, Wilmington, DE, USA*

Abstract

First-principles density functional (DFT) quantum chemical calculations were carried out to understand the overall energetics for the hydrogenation of maleic anhydride to tetrahydrofuran (THF), over a Pd(1 1 1) cluster model. The calculated vapor phase structures and vibrational frequencies for maleic anhydride, succinic anhydride, γ-butyrolactone and THF compare well with the reported experimental X-ray crystal structure data and infrared (IR) frequency measurements. The overall reaction energies for vapor phase maleic anhydride hydrogenation to THF, determined using DFT, are within 5 kcal/mol of the enthalpies of reaction, based on standard heats of formation. The adsorption structures for maleic anhydride, succinic anhydride, γ-butyrolactone, THF, water and atomic hydrogen were completely optimized on a fixed Pd(12,7) cluster model of the Pd(1 1 1) surface. The binding energies for maleic anhydride on the Pd_{19} cluster in the di-σ, π and η^1 adsorption modes were −83, −34 and −28 kJ/mol, respectively. The computed adsorption energy and vibrational frequencies for di-σ bound maleic anhydride on Pd(1 1 1) are in good agreement with temperature-programmed desorption (TPD) and high-resolution electron energy loss spectroscopy (HREELS) measurements of Xu and Goodman [Langmuir 12 (1996) 1807-1816]. Preliminary calculations indicate that the most favorable adsorption mode for succinic anhydride, γ-butyrolactone, THF and water on Pd(1 1 1) is η^1, with binding energies of −28, −38, −45 and −30 kJ/mol, respectively. The energetically most stable adsorption site for atomic hydrogen on the Pd(1 1 1) surface is the 3-fold fcc site, with a binding energy of −257 kJ/mol. Towards understanding the detailed reaction mechanism on Pd(1 1 1), we have postulated elementary reaction pathways for C–H bond formation in maleic anhydride hydrogenation and the ring opening reaction of maleic anhydride on Pd(1 1 1). The DFT-computed activation barrier for C–H bond formation in maleic anhydride hydrogenation to maleic anhydryl on a Pd_{19} cluster is +82 kJ/mol and the energy of reaction is −9 kJ/mol. The ring opening reaction of maleic anhydride on Pd(1 1 1) has an activation barrier of +163 kJ/mol and is endothermic by 90 kJ/mol. The activation barrier on Re(0 0 0 1), however, is only +80 kJ/mol, whereas the reaction is exothermic by −96 kJ/mol. These results are consistent with the observations from UHV experiments.

Keywords: Selective hydrogenation; Maleic anhydride; Tetrahydrofuran

1. Introduction

Tetrahydrofuran (THF), an important intermediate in the manufacture of polyurethane elastomers and the

*Corresponding author. Tel.: +1-804-924-6248; fax: +1-804-982-2658; e-mail: mn4n@virginia.edu

0920-5861/99/$ – see front matter
PII: S0920-5861(98)00493-3

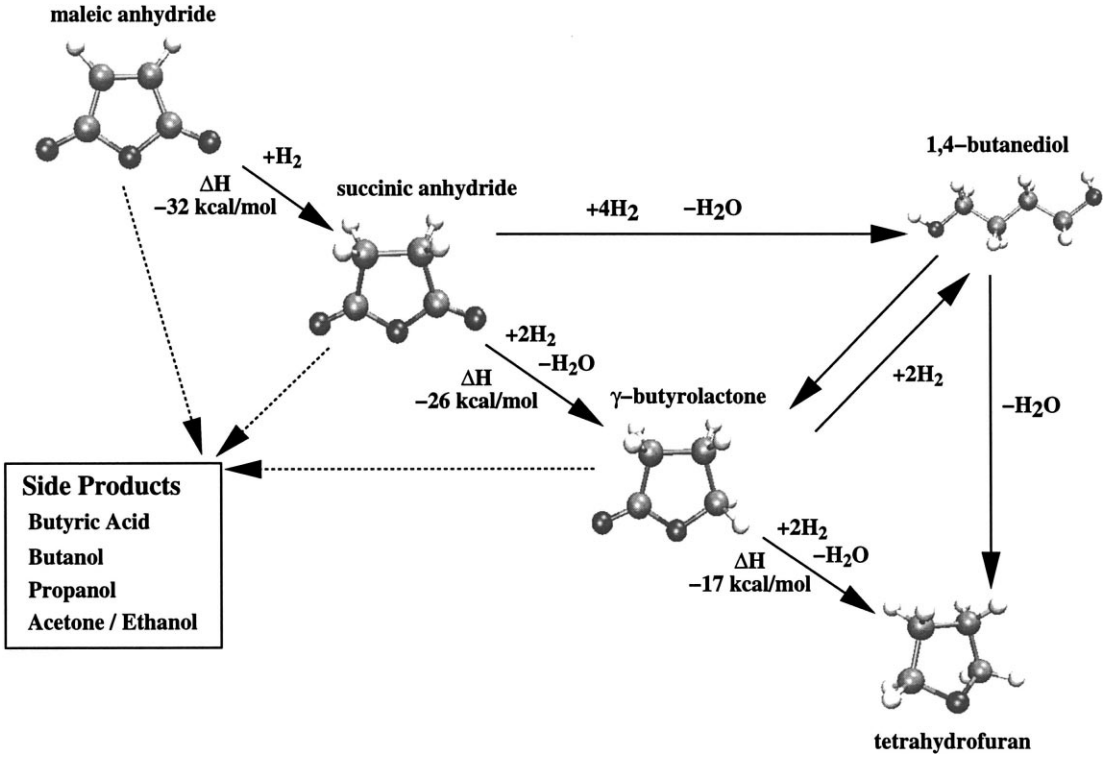

Fig. 1. Overall reaction pathway generally proposed for the hydrogenation of maleic anhydride to THF [4].

spandex fibre Lycra[1], is commercially produced by the hydrogenation of maleic anhydride over a bimetallic Pd–Re based catalyst [2,3]. The single stage hydrogenation reaction is actually composed of various serial and parallel reaction steps. A general mechanism for the hydrogenation of maleic anhydride, in the vapor phase, over Cu–chromite catalysts was proposed by Messori and Vaccari [4] and is shown in Fig. 1. The first reaction step involves the hydrogenation of the C=C bond of maleic anhydride to produce succinic anhydride. Subsequently, the C=O groups are hydrogenated to give γ-butyrolactone and THF. 1,4-Butanediol, a secondary product of the reaction, is postulated to be formed directly from THF, γ-butyrolactone or succinic anhydride. Undesired straight chain alkanes, alcohols and acids are produced by overhydrogenation and hydrogenolysis reactions. Although there is ample experimental evidence supporting this overall reaction network, there is limited understanding of the mechanism and the elementary kinetic steps involved. In addition, multifunctional adsorbates such as maleic anhydride, can bind to a metal surface in a variety of ways, in which the C=C or C=O moieties are favorably aligned. This leads to a number of competing elementary surface reaction steps, obscuring the governing mechanism. Inadequate knowledge of the microkinetic steps involved in the reaction has, in part, precluded identifying the key factors that control the activity and intermolecular selectivity of the bimetallic catalyst. To begin to address these issues, we are examining the catalytic reaction chemistry at a fundamental level using theoretical quantum chemical methods, in conjunction with ultra-high vacuum (UHV) single crystal experiments.

As a first step towards elucidating the reaction mechanism, we set out to determine the adsorption energetics and overall reaction energies on well-defined surfaces by closely coupling theory and experiment. First-principle quantum chemical density functional theory (DFT) calculations were used to probe the fundamental chemisorption and surface

[1]E.I. DuPont de Nemours and company.

chemical reactivity of the principal intermediates in maleic anhydride hydrogenation on model transition metal clusters and extended surfaces. Non-local DFT calculations provide reliable structural, energetic and spectral information that are available for direct comparison with ultra high vacuum (UHV) surface science experiments on pristine single crystal surfaces [5]. The UHV experiments were performed at DuPont and are the subject of a forthcoming communication [6].

In this paper, we examine the binding of the reactants, products and intermediates on model palladium clusters and compute the overall energetics of the principal steps involved in a postulated catalytic cycle. Comparison is drawn with the experimental values wherever available. A comprehensive analysis of the vapor phase intermediates is also carried out to ensure reliable surface energetic predictions.

2. Computational details

All results reported in this paper were obtained using non-local density functional theory (DFT) calculations, as implemented in the linear combination of contracted Gaussian type orbitals (LCGTO) based code DGauss [7–9]. The exchange–correlation potential used in the local-spin density approximation was that of Vosko et al. [10]. In addition, non-local gradient corrections, due to Becke (for exchange) and Perdew (for correlation) [11–13], were incorporated in the exchange–correlation potential within the self-consistent-field (SCF) procedure. Double zeta valence basis sets, which were optimized for DFT calculations [14], were used to describe the atomic orbitals for carbon, hydrogen and oxygen. Relativistic effects are important for modeling the core electrons of transition metals such as palladium. In all our calculations, relativistic effects were partly accounted for, by the use of a scalar relativistically corrected pseudopotential to represent the inner-shell electronic states of palladium [15,16]. Freezing of the core electrons by the construction of a pseudopotential also minimizes the computational effort during the self-consistent-field procedure.

Binding energies for the adsorbates were calculated using 19 atom Pd(12,7) clusters to represent the Pd(1 1 1) surface. To determine the ground state geometry, the cluster was constrained to the bulk geometry while the adsorbate was completely optimized. In previous work, we demonstrated that complete optimization of the cluster can change the energetics of adsorption by about 20–30 kJ/mol [5]. Such relaxations are in part due to the incomplete coordination of the edge metal atoms of the cluster and are more pronounced for atomic adsorbates such as O, that have very high binding energies [5]. Binding energy calculations on the constrained Pd(12,7) cluster give reliable estimates of the adsorption energy on the periodic Pd(1 1 1) surface [5]. The reported binding energies are calculated as

$$\Delta E_{\text{ads}} = E_{\text{cluster–adsorbate}} - E_{\text{cluster}} - E_{\text{adsorbate}},$$

where $E_{\text{cluster–adsorbate}}$ is the total energy of the optimized ground state of the adsorbate on the metal cluster, E_{cluster} is the total energy of the bare Pd_{19} cluster and $E_{\text{adsorbate}}$ is the total energy of the adsorbate in the ground state.

The effect of spin multiplicity on chemisorption energy was examined for maleic anhydride adsorption on a Pd_3 cluster. Changing the spin multiplicity from a singlet (spin-restricted) to a triplet (spin-unrestricted) was observed to change the adsorption energy by 35 kJ/mol. All calculations reported in this paper were therefore performed spin-unrestricted. The most favorable multiplicity for the bare Pd(12,7) cluster was determined to be the triplet. The adsorption of the intermediate did not appear to change the spin multiplicity of the system. This was verified for a number of individual cases. The spin multiplicity of the bare cluster was therefore used for the cluster/adsorbate system. The effect of basis-set superposition error (BSSE) was studied for maleic anhydride di-σ adsorption on a palladium dimer. Inclusion of BSSE was found to change the adsorption energy by less than 5 kJ/mol and was therefore neglected in the present study. All SCF calculations were converged to within 1.0×10^{-4} a.u. for the charge density and 1.0×10^{-6} a.u. for the energy. All structures were optimized to within 3.0×10^{-3} a.u./Å for the gradient.

3. Results and discussion

3.1. Vapor phase structures

The ground state structures for vapor phase maleic anhydride, succinic anhydride, γ-butyrolactone and

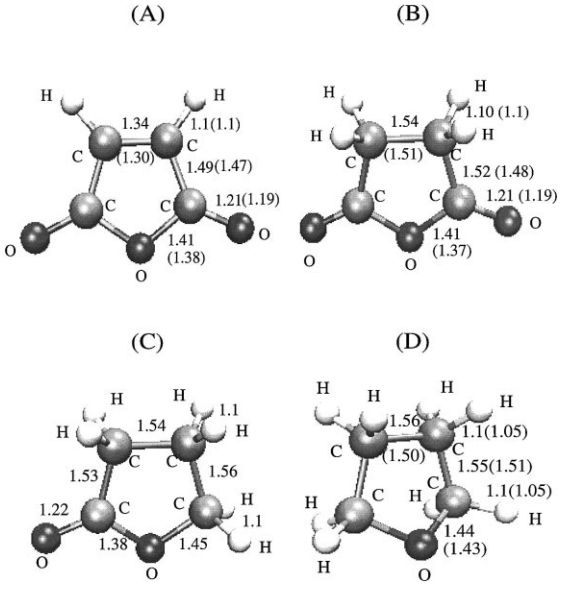

Fig. 2. Ground state structures of (a) maleic anhydride; (b) succinic anhydride; (c) γ-butyrolactone and (d) tetrahydrofuran. Numbers in parenthesis are X-ray crystal structure data obtained from the Cambridge Crystal Structure Database [17].

tetrahydrofuran were computed by unconstrained geometry optimization using non-local DFT calculations. The optimized structures are shown in Fig. 2. Calculations suggest that all of the carbon and oxygen atoms in maleic and succinic anhydride are coplanar in the ground state and the molecules have C_{2V} point group symmetry. The carbon and oxygen atoms in γ-butyrolactone are also coplanar but the molecule only has C_S symmetry in the lowest energy conformation. The planar structure of maleic anhydride, succinic anhydride and γ-butyrolactone are attributed to the sp^2 hybridization of orbitals on the ring oxygen and the carbon atoms of the C=O groups. This hybridization stabilizes the structure by allowing the delocalization of the π-electrons over the O=C–O–C=O group in both maleic and succinic anhydride and the O=C–O group in γ-butyrolactone. The minimum energy conformation for THF, on the other hand, is non-planar, with the ring oxygen displaced outside the plane of the four carbon atoms. The valence orbitals on the carbon atoms and ring oxygen, in this case, are sp^3 hybridized and the molecule has C_S symmetry.

The known X-ray crystal structural data for maleic anhydride, succinic anhydride and tetrahydrofuran are also depicted in Fig. 2, to compare with our DFT-optimized structures [17]. Nearly all the optimized bond distances are within 0.04 Å of the corresponding experimental value. For THF, the computed bond distances were slightly longer than that known from the X-ray data. Specifically, the βC–βC bond length (1.56 Å) is longer than the corresponding distance in the crystalline state by about 0.06 Å. The computed value is closer to the known C–C single bond distance for vapor phase ethane (1.54 Å). It is important to note that the X-ray crystal structures are determined in the crystalline state, where crystal packing and other short-range intermolecular forces such as H-bonding may potentially distort the molecule. Our DFT-optimized geometries for the isolated molecules would be more characteristic of vapor phase structures. A more appropriate test of the DFT-computed geometry would, therefore, be to compare it with the vapor phase structure or to match structure dependant properties of the molecule, such as the vapor phase infrared (IR) vibrational frequencies.

3.2. Infrared vibrational spectra

To further examine the accuracy of the DFT-predicted structures, vibrational frequencies were computed for the ground state structures. Second derivative frequency calculations on each of the ground state structures confirmed that the geometry optimizations have located minima on the potential energy hypersurface. The normal vibrational modes for maleic anhydride, succinic anhydride, γ-butyrolactone and THF are tabulated in Table 1. Experimentally measured IR frequencies are also provided for comparison. The vibrational frequencies for vapor phase maleic anhydride are from Mirone and Chiorboli [18]. The frequencies for succinic anhydride, γ-butyrolactone and THF are from the Aldrich Library of FT-IR spectra [19].

The computed C=C stretch frequency for vapor phase maleic anhydride is 1620 cm^{-1}. This mode has a low intensity in the vapor phase IR spectrum of maleic anhydride due to the small dipole moment change associated with this stretch. A comparison with the calculated C=C stretch frequency, 1332 cm^{-1} (IR invisible) for gas phase ethylene indicates that this mode is blue-shifted in maleic anhydride. This is in consonance with the observation that

Table 1

Experiment (cm^{-1})	DFT (cm^{-1})	Mode assignment
Infrared vibrational frequencies for maleic anhydride		
558	535	C=O bending in-plane
699	683	Ring distortion in-plane
840	800	C–H bending out-of-plane
893	858	C–O stretch
1057	1038	C–C+C–O–C asymmetric stretch
1064	1053	C–H bending in-plane
1231	1235	C–C+C–O–C symmetric stretch
1602	1618	C=C stretch (low intensity)
1801	1785	C=O asymmetric stretch
1852	1844	C=O symmetric stretch
3175	3179	C–H stretch
Infrared vibrational frequencies for succinic anhydride		
563	650	Ring distortion in-plane
818	868	C–O stretch
914	998	C–C stretch
1052	1026	C–C+C–O–C asymmetric stretch
1211	1193	C–C+C–O–C symmetric stretch
1279	1247	C–O–C symmetric stretch+C–C stretch
1419	1436	H–C–H scissoring action
1785	1805	C=O asymmetric stretch
1861	1876	C=O symmetric stretch
Infrared vibrational frequencies for γ-butyrolactone		
867	818	Ring distortion in-plane
1049	992, 1042	C–C+ring C–O stretch
1161	1153, 1162	C–C+ring C–O stretch
1380	1390	C–H out-of-plane bending
1824	1801	C=O stretch
2910, 2993	3007, 3025, 3033	C–H stretch
Infrared vibrational frequencies for tetrahydrofuran		
919	898	C–C symmetric stretch
1085	1057	C–O–C asymmetric stretch
1176	1177	C–H out-of-plane symmetric bending
1464	1475	H–C–H scissoring action
2870	2921, 2928	α C–H stretch
2982	3002, 3012	β C–H stretch

π-electron delocalization between the C=O groups and the C=C groups has an effect of strengthening the C=C bond in maleic anhydride relative to ethylene. The C=C bond distance (1.34 Å) in maleic anhydride, however, is similar to that computed for vapor phase ethylene. The C–C bond distance and vibrational frequency for succinic anhydride, γ-butyrolactone and THF are almost identical to that calculated for ethane (C–C bond distance=1.54 Å; ν_{c-c}=1000 cm^{-1}). The C=O stretch frequency for maleic anhydride, succinic anhydride and γ-butyrolactone are determined to be about 1800 cm^{-1} and are consistent with experiment. The DFT-computed vibrational frequencies depicted in Table 1 are within 5% of the experimental vibrational spectra, thus helping to confirm the ground state structures for maleic anhydride and the other vapor phase intermediates.

3.3. Vapor phase reaction energies

Based on the total SCF energies of the structures that were outlined in Fig. 1, we have calculated the overall vapor phase energies of reaction for many of the principal reaction steps in the hydrogenation of maleic anhydride. It is important to note that quantum-chemical reaction enthalpies are fundamentally different from the SCF-based reaction energies [20,21]. Theoretical calculation of reaction enthalpy requires the inclusion of zero-point energy correction terms and specific heats of reactant and product species. These terms are determined by performing a vibrational frequency calculation for each of the structures at the ground state. Details on computation of reaction enthalpies and free energies for maleic acid hydrogenation are presented elsewhere [21]. In this paper we compare the DFT-computed energy of reaction (based on the total SCF energy) and the experimental enthalpies of reaction (computed from the standard enthalpy of formation of the compounds in the vapor phase at 298 K). All the hydrogenation steps in the reaction sequence are exothermic. The hydrogenation of the C=C bond has the highest exothermicity of about 30 kcal/mol. There is a successive decrease in the reaction exothermicity as the C=O groups are hydrogenated to form γ-butyrolactone and THF. The dehydration of 1,4-butanediol to tetrahydrofuran is observed to be almost thermoneutral. It is seen that the calculated energies of reaction are predicted to within 1 kcal/mol of the experimental value, except for the hydrogenation of maleic anhydride to succinic anhydride, where the difference is about 4 kcal/mol (cf. Table 2).

3.4. Chemisorption on Pd(1 1 1)

Multifunctional adsorbates such as maleic anhydride can bind to metal surfaces in various different

Table 2
Reaction energetics for vapor phase hydrogenation of maleic anhydride

Reaction	DFT ΔE_0 reaction (kcal/mol)	$\Delta H_{r\times n}$ (experiment) based on ΔH_f^0 at 298 K[a] (kcal/mol)
$C_4H_2O_{3\,\text{maleic anhydride}} + H_2 = C_4H_4O_{3\,\text{succinic anhydride}}$	−35.19	−30.9
$C_4H_4O_{3\,\text{succinic anhydride}} + 2H_2 = C_4H_6O_{2\,\gamma\text{-butyrolactone}} + H_2O$	−20.0	−19.2
$C_4H_6O_{2\,\gamma\text{-butyrolactone}} + 2H_2 = C_4H_8O_{\text{tetrahydrofuran}} + H_2O$	−13.6	−14.2
$C_4H_6O_{2\,\gamma\text{-butyrolactone}} + 2H_2 = C_4H_{10}O_{2\,1,4\text{-butanediol}}$	−14.3	−14.9
$C_4H_{10}O_{2\,1,4\text{-butanediol}} = C_4H_8O_{\text{tetrahydrofuran}} + H_2O$	+0.6	+0.6
$C_4H_2O_{3\,\text{maleic anhydride}} + 5H_2 = C_4H_8O_{\text{tetrahydrofuran}} + 2H_2O$	−68.8	−64.3

[a] Standard heats of formation are from the CRC Handbook of Chemistry and Physics [22].

conformations, providing multiple surface reaction channels that ultimately control the reaction selectivity. It is therefore essential to understand the fundamental interactions that control chemisorption. By examining numerous possible orientations, we have identified three principal modes for the chemisorption of maleic anhydride on transition metal surfaces. They are defined as

atop η^1 binding through the ring oxygen; the molecular plane of maleic anhydride is oriented parallel to the surface normal

di-σ η^2 binding of maleic anhydride via two σ bonds through the ethylenic moiety; the molecular plane being nearly parallel to the surface

π η^1 binding of maleic anhydride via a π bond through the ethylenic moiety; the molecular plane, again, being parallel to the surface. For the π adsorption mode there may be additional interactions of the C=O groups with the surface.

These three adsorption configurations for maleic anhydride on a model Pd(12,7) cluster are depicted in Fig. 3.

Our results indicate that the preferred mode of chemisorption of maleic anhydride on Pd(1 1 1), at low coverage, is di-σ, with a binding energy of −83 kJ/mol. The atop chemisorption mode is least favorable and has a binding energy of −28 kJ/mol. π adsorption of maleic anhydride has a binding energy of −34 kJ/mol, which is comparable to that of the atop mode but substantially lower than that for di-σ adsorption. The results of UHV temperature-programmed desorption experiments of maleic anhydride from Pd(1 1 1) find that the energy of desorption is about 90 kJ/mol [6]. In a follow up paper, Xu and Goodman [1] published the temperature-programmed desorption (TPD) spectra for maleic anhydride from the Pd(1 1 1), monolayer Pd(1 1 1)/Mo(1 1 0) and Mo(1 1 0) surfaces. Molecular desorption of maleic anhydride from Pd(1 1 1) surfaces was reported to peak at a temperature of 374 K. Assuming a first-order desorption process, with $\nu = 1\times10^{13}\ s^{-1}$ for the Redhead equation [23], the binding energy of maleic anhydride on Pd(1 1 1) is estimated to be about −93 kJ/mol. This is in good agreement with the DFT-predicted value of −83 kJ/mol.

To determine whether the optimized geometry identified here is truly the lowest energy conformation, we have calculated the vibrational frequencies for maleic anhydride bound to Pd(1 1 1) in the di-σ and π adsorption modes and compared them with the high resolution electron energy loss spectroscopy (HREELS) spectra of Xu and Goodman [1], measured at subsaturation coverage. Based on their HREELS and TPD data, Xu and Goodman [1] speculated the formation of di-σ bound maleic anhydride on Pd(1 1 1) and π-bound maleic anhydride on monolayer Pd(1 1 1)/Mo(1 1 0). In Table 3, we have compared the calculated and experimental values of the principal vibrational modes of maleic anhydride chemisorbed in the π and di-σ configuration on Pd(1 1 1) surfaces.

The distinguishing features in the vibrational spectra for π and di-σ chemisorption modes are in the C–H bending, C–H stretch, C–O–C stretch and C=C stretch frequencies. sp^3 hybridization of the carbon atoms of the C=C bond for di-σ adsorption lowers the *s*-character in the C–H bond, resulting in a slight red-shift in

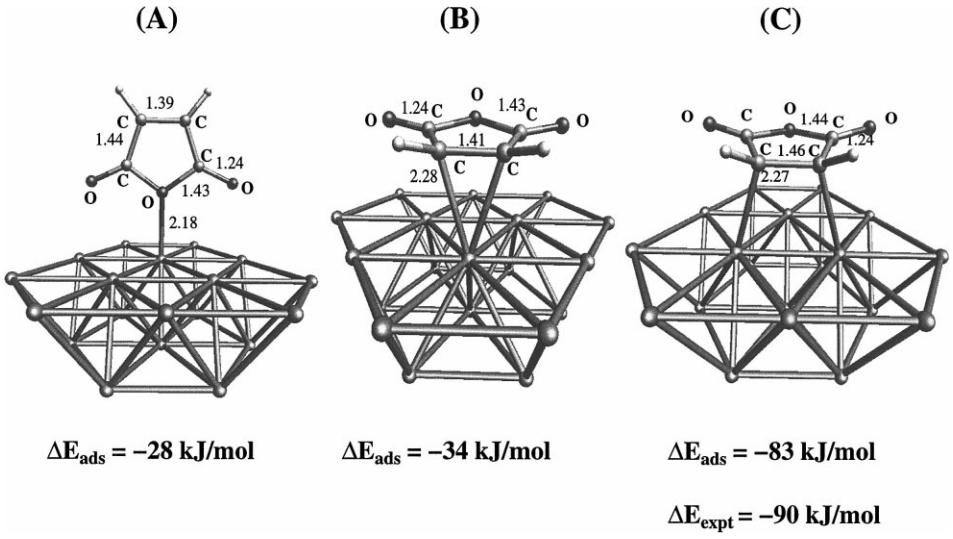

Fig. 3. Adsorption modes and energetics for maleic anhydride on model Pd(1 1 1) clusters: (A) η^1 adsorption; (B) π adsorption; (C) di-σ adsorption.

Table 3
Vibrational frequencies for π and di-σ bound maleic anhydride on Pd(1 1 1)

Mode	Experiment[a] $Pd(1\,1\,1)_{ML}/Mo(1\,1\,0)$	DFT calculated π maleic on Pd(1 1 1)	Experiment[a] Pd(1 1 1) multilayer	DFT calculated di-σ maleic on Pd(1 1 1)
C=O in-plane bend	400	510	400	423
Ring bending in-plane	680	700	690	682
C–H bend out-of-plane	990	1000	800	836
C–C stretch	–	841	–	879
C–O–C symmetric stretch	1175	1151	1200	1228
C=C stretch	1300	1664	Not seen	1022
C=O stretch	1620	1856	1780	1821
C–H stretch	3045	3200	2995	3150

[a] From ref. [1].

the C–H stretch frequency relative to vapor phase and π-bound maleic anhydride. The most significant differences between π and di-σ maleic anhydride on Pd(1 1 1) are in the C=C stretch frequency. Unfortunately, this mode has a very low intensity in the EELS spectrum of maleic anhydride on Pd and was not measured for the di-σ mode. From Table 3, it is clear that there are significant differences between the computed and experimental C=C and C=O stretch frequencies for π-bound maleic anhydride. It is important to note that our computations are representative of π-bound maleic anhydride on the Pd(1 1 1) surface and not the pseudomorphic overlayer of Pd(1 1 1) on Mo(1 1 0). Our calculations indicate negligible interaction of the C=O groups with the surface for both di-σ and π-bound maleic anhydride on Pd(1 1 1). There are little differences, therefore, in our computed C=O stretch frequencies for the di-σ and π adsorption modes. The C=C bond interaction with the surface is also weak for π adsorption, as is evident from the low chemisorption energy computed by DFT and the small perturbation in the C=C stretch frequency from vapor phase maleic anhydride ($1600\,cm^{-1}$). For metals such as Re(0 0 0 1), however, our calculations show a significant overlap of the C=O group orbitals with the d-orbitals of the surface metal atoms for π

adsorption [24] resulting in a substantial stretch of the C=O bond. It is likely that such strong interactions of the C=O and C=C groups of π-bound maleic anhydride also exist for the monolayer Pd(1 1 1) on Mo(1 1 0) surface and are responsible for the significantly red-shifted C=O and C=C stretch frequencies, measured by Xu and Goodman [1] on this surface. This is also consistent with the fact that the binding energy of π-bound maleic anhydride on monolayer Pd(1 1 1) on Mo(1 1 0) (-90 kJ/mol), measured by Xu and Goodman [1], is substantially higher than our computed chemisorption energy for π-bound maleic anhydride on Pd(1 1 1) (-34 kJ/mol).

It is verified that the DFT-computed vibrational frequencies for di-σ bound maleic anhydride on Pd(1 1 1) are within 5% of the experimental values (Table 3). As mentioned earlier, there are differences between the vibrational frequencies for π-bound maleic anhydride on Pd(1 1 1) and the HREELS frequencies of Xu and Goodman for maleic anhydride on the bimetallic, monolayer Pd(1 1 1)/Mo(1 1 0) system. The adsorption geometry of maleic anhydride on the monolayer Pd(1 1 1)/Mo(1 1 0) system, therefore, cannot be confirmed at this stage. Our results illustrate how DFT in conjunction with surface science probe techniques, such as TPD and EELS, can be an invaluable tool in the identification of the geometry of multifunctional adsorbates on surfaces. A more detailed analysis of maleic anhydride chemisorption on various transition metals will be presented in a forthcoming paper [24].

An important observation from Fig. 3 is that atop chemisorption of maleic anhydride has a binding energy less than that for the di-σ or π adsorption modes. The η^1 mode, however, requires a smaller surface ensemble for adsorption than the π or di-σ modes. At higher surface coverages of maleic anhydride, lateral adsorbate–adsorbate repulsion effects become important. The atop adsorption mode may be favored at higher surface coverages. Similar changes in adsorption configuration with change in surface coverage have been reported for analogous olefinic ring structures such as 2,5-dihydrothiophene on Mo(1 1 0) [25]. HREELS measurements on Mo(1 1 0) have demonstrated that at low coverages, 2,5-dihydrothiophene lies nearly parallel to the surface, but at higher coverages it sits atop and nearly perpendicular to the Mo(1 1 0) surface [25].

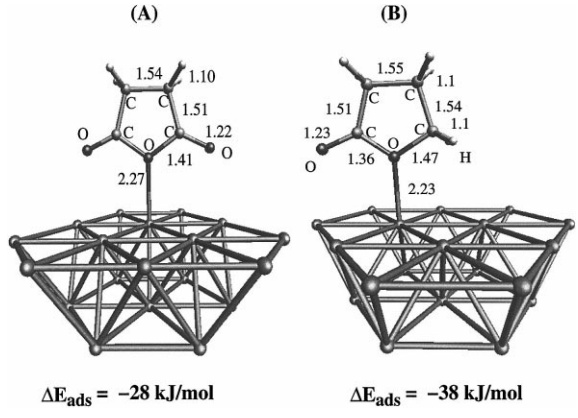

Fig. 4. Non-local DFT-optimized structures on model Pd(1 1 1) clusters: (A) succinic anhydride and (B) γ-butyrolactone.

Preliminary calculations on the adsorption of succinic anhydride, γ-butyrolactone and tetrahydrofuran on Pd(1 1 1) suggest that the atop mode is the only stable molecular adsorption mode for these species on Pd(1 1 1) surfaces. The adsorption is, therefore, significantly weaker than that of maleic anhydride on Pd(1 1 1). The optimized geometry for the intermediates bound to a Pd(12,7) cluster are shown in Figs. 4–6. The DFT-computed binding energy of succinic anhydride, γ-butyrolactone and THF on Pd(1 1 1) are -28, -38 and -45 kJ/mol, respectively. TPD measurements at UHV conditions indicate that the adsorption energies for succinic anhydride and

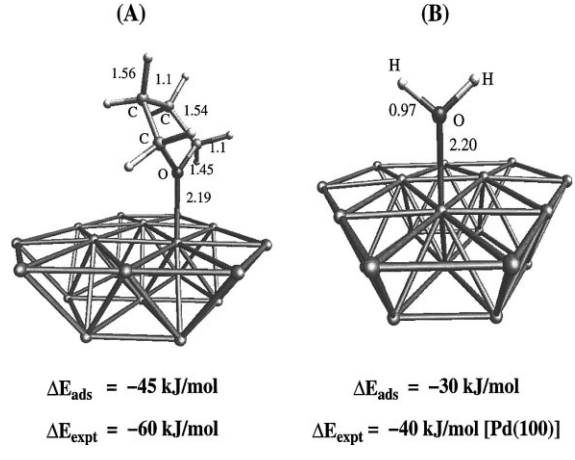

Fig. 5. Non-local DFT-optimized structures on model Pd(1 1 1) clusters: (A) tetrahydrofuran and (B) water.

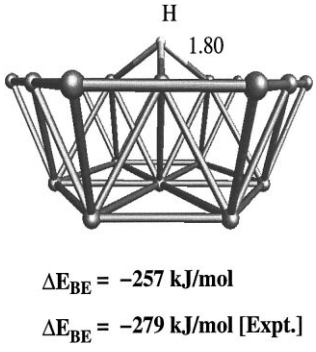

Fig. 6. Non-local DFT-optimized geometry of atomic hydrogen on a model Pd(12,7) cluster.

THF are on the order of −45 kJ/mol [6]. The DFT-computed binding energy for THF is in good agreement with experimental measurement. The binding energy of succinic anhydride, however, is slightly lower than the value measured experimentally, but within the limits of accuracy of the DFT methodology [5]. The computed binding energy of succinic anhydride is comparable to that of maleic anhydride in the atop mode. There is a slight increase in the atop adsorption energy as the C=O groups of succinic anhydride are hydrogenated. Calculations indicate that the molecular orientation of succinic anhydride and γ-butyrolactone for atop adsorption on Pd(1 1 1) is such that the plane of the molecules is parallel to the surface normal. For THF, the molecule is tilted away from the surface normal by about 6° (Fig. 5). The adsorption geometry can be rationalized on the basis of the orientation of the hybridized valence orbitals on the ring oxygen atom as determined from valence shell electron pair repulsion theory.

The overall heats of surface reaction on Pd(1 1 1) were computed from the energies for structurally optimized H_2O and atomic H on the Pd(12,7) cluster. The optimized structures are shown in Figs. 5 and 6, respectively. The binding energies of H_2O and H on the Pd(1 1 1) surface were computed from DFT calculations to be −30 and −257 kJ/mol, respectively. The energetically favorable adsorption site for H on the Pd(1 1 1) surface, is the 3-fold fcc site [26–30]. Since the binding energy of H_2 in the gas phase is −436 kJ/mol [19], the heat of dissociative adsorption of H_2 on Pd(1 1 1) is calculated to be about −78 kJ/mol. Our calculated binding energy for H on Pd(1 1 1) is in good agreement with the reported theoretical and experimental values [26–30]. Water binds atop, through the oxygen, with the plane of the molecule tilted away from the surface normal, similar to that of THF, as depicted in Fig. 5. On clean Pd(1 0 0) surfaces, the binding energy of molecularly adsorbed H_2O is estimated to be about −40 kJ/mol, based on experimental TPD data [31]. On a more close packed Pd(1 1 1) surface, it is likely that the magnitude of the binding energy of water will be lower and in better agreement with our predicted adsorption energy of −30 kJ/mol.

Having determined the gas phase energies as well as the binding energies of the principal reactant, intermediate and product species on Pd(1 1 1), we can now compute the overall energetics for the hydrogenation of maleic anhydride on a model Pd(12,7) cluster. Our DFT results were used to construct the reaction energy diagram for maleic anhydride hydrogenation on Pd(1 1 1) depicted in Fig. 7. Calculations indicate that the surface reaction step for the hydrogenation of maleic anhydride to succinic anhydride is mildly exothermic [$\Delta E_{r\times n}$=−14 kJ/mol]. The heat liberated in the overall surface reaction to form succinic anhydride is 133 kJ/mol lower than that in the vapor phase. Interestingly, the surface reaction steps, on Pd(1 1 1), of hydrogenation of succinic anhydride to γ-butyrolactone, and γ-butyrolactone to THF, are endothermic by 32 and 63 kJ/mol, respectively. The corresponding vapor phase energies of reaction for these hydrogenation steps are −84 kJ/mol (exothermic) and −57 kJ/mol (exothermic), respectively. This significant difference between vapor phase and surface reaction energetics is due to the extremely strong adsorption energy of the reactants (principally atomic hydrogen) and the weak adsorption energy of the product species on the Pd(1 1 1) surface. The net heat liberated in the overall catalytic cycle for the hydrogenation of maleic anhydride to THF is calculated to be 288 kJ/mol.

4. Towards understanding the mechanism for maleic anhydride hydrogenation

Individual steps in the mechanism are being examined in more detail by performing extensive reaction coordinate calculations. By probing the potential energy hypersurface connecting the reactant and pro-

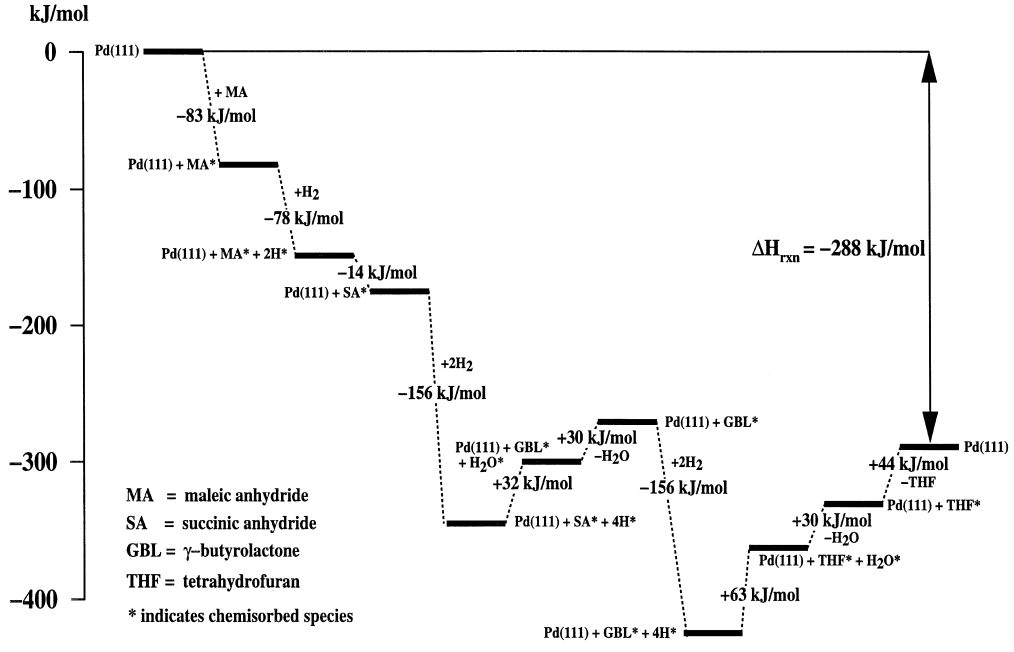

Fig. 7. Reaction energy diagram for the hydrogenation of maleic anhydride on Pd(1 1 1).

duct species, we have located transition states and computed activation barriers for some of the elementary catalytic reactions, using the principles of transition state theory.

The hydrogenation of the C=C bond of maleic anhydride on Pd(1 1 1) is postulated to proceed via a Horiuti–Polanyi mechanism [32], similar to that for ethylene hydrogenation. Fig. 8 depicts the surface reactant, transition state and product state for the initial addition of atomic hydrogen to adsorbed maleic anhydride to form the maleic anhydryl intermediate. We have also examined other C=C bond hydrogenation reactions on Pd(1 1 1) by probing the reverse reaction of β-hydride elimination [5]. By studying various possible substituents on the carbon atom, we have analyzed the effect of different electron withdrawing substituents on the activation barrier for β-hydride elimination (or the reverse C–H bond formation step) [5]. Our results indicate that the presence of stronger electron withdrawing substituents raise the barrier for β-hydride elimination [5,33]. A more detailed discussion of maleic anhydride C=C bond hydrogenation will be presented in a forthcoming paper [33].

The formation of straight chain alcohols, acids and aldehydes during the hydrogenation reaction results in the loss of selectivity to THF. These species are formed by the catalytic ring opening of maleic anhydride and the other cyclic intermediates. Our TPD studies of maleic anhydride on Re(0 0 0 1) [6] along with those of Xu and Goodman [1] for Mo(1 1 0) indicate that maleic anhydride readily ring opens to form oxametallacycle intermediates. Such ring opening reactions are not observed on Pd(1 1 1) surfaces. To understand this behavior, we used theory to analyze the mechanism of ring opening of maleic anhydride on Pd(1 1 1) and Re(0 0 0 1) surfaces. Our calculations suggest that the reaction coordinate from the atop adsorption mode involves tilting of the adsorbed maleic towards the surface along with a stretching of the ring C–O bond. In essence, this allows a surface metal atom to insert into the ring C–O bond to form a surface oxametallacycle. The resulting oxametallacycle complex is shown in Fig. 9. On Pd(1 1 1), the ring opening of maleic anhydride is highly endothermic (+90 kJ/mol) with an activation energy of +163 kJ/mol. The high barrier along with the endothermicity makes this an unlikely path on

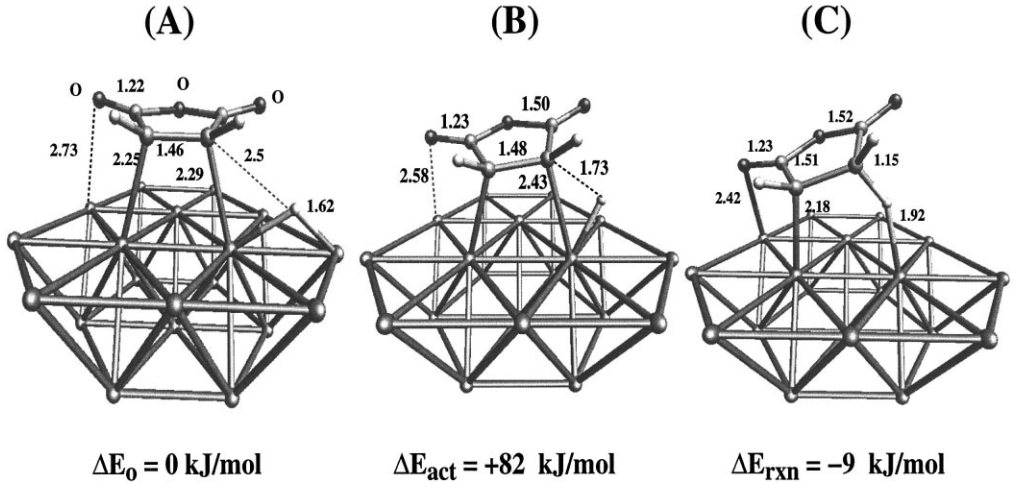

Fig. 8. Reaction pathway in the vapor phase hydrogenation of maleic anhydride to maleic anhydryl on Pd(1 1 1): (A) di-σ bound maleic anhydride and H adsorbed on adjacent site; (B) transition state; (C) maleic anhydryl on Pd(1 1 1).

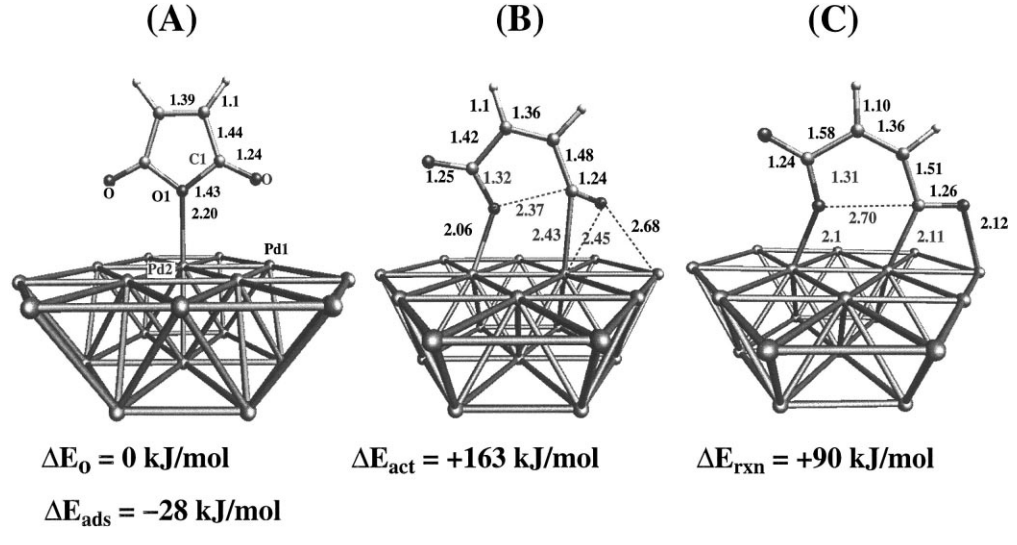

Fig. 9. Reaction pathway in the ring opening reaction of maleic anhydride on Pd(1 1 1): (A) η^1 bound maleic anhydride on Pd(1 1 1); (B) transition state; (C) ring-opened oxametallacycle intermediate on Pd(1 1 1).

Pd(1 1 1). On the other hand, the calculations show that the reaction has a low activation barrier (+80 kJ/mol) and is highly exothermic (−96 kJ/mol) on Re(0 0 0 1) surfaces. Coupled with the fact that the atop chemisorption energy for maleic anhydride on Re(0 0 0 1) is −172 kJ/mol (DFT-computed), the ring opening reaction is non-activated on Re(0 0 0 1), consistent with our experimental TPD observations [6].

5. Conclusions

The overall energetics for the selective hydrogenation of maleic anhydride to THF over Pd(1 1 1) was examined using non-local DFT calculations. The DFT-optimized vapor phase structure and vibrational frequencies for maleic anhydride, succinic anhydride, γ-butyrolactone and THF are in good agreement with

reported experimental X-ray crystal structures and IR frequency measurements. The overall energies of reaction for the vapor phase hydrogenation of maleic anhydride to THF were also computed. The gas phase maleic anhydride C=C and C=O group hydrogenation steps are exothermic and are observed to be within 5 kcal/mol of the experimental estimates of the heats of reaction, based on the standard enthalpies of formation.

Towards elucidating the reaction mechanism and energetics for maleic anhydride hydrogenation on Pd catalysts, we have optimized the structures of the principal reactant and product species on well-defined, 19 metal atom Pd(12,7) clusters. The adsorption of maleic anhydride in different modes such as η^1, di-σ and π, were critically examined. Di-σ adsorption of maleic anhydride, through the C=C moiety, was found to be the most favorable adsorption mode at low coverage, with a binding energy of -83 kJ/mol. The π and η^1 adsorption modes have significantly lower binding energies of -34 and -28 kJ/mol, respectively. Vibrational frequencies were also computed for di-σ and π-bound maleic anhydride on Pd(1 1 1). The adsorption energy and vibrational frequencies for di-σ bound maleic anhydride compare well with experimental TPD and HREELS measurements of Xu and Goodman [1], confirming the adsorption geometry of maleic anhydride on Pd(1 1 1), at low surface coverage. DFT calculations indicate that succinic anhydride, γ-butyrolactone, THF and water bind atop to the Pd(1 1 1) surface. The adsorption energy for succinic anhydride is -28 kJ/mol, which is identical to the η^1 adsorption energy of maleic anhydride, but is slightly lower than the experimental adsorption energy estimated from TPD data [6]. The DFT-calculated chemisorption energy of THF and water on Pd(1 1 1) are -45 and -30 kJ/mol, respectively, and are within 10 kJ/mol of the experimentally measured binding energy [6,31]. The energetically most favorable adsorption site for atomic hydrogen on Pd(1 1 1), is the 3-fold fcc site, with a binding energy of -257 kJ/mol. Using this binding energy, the heat of dissociative adsorption of H_2 on Pd(1 1 1) is calculated to be -78 kJ/mol.

Based on the DFT-computed adsorption structures and chemisorption energies, we have determined the overall energies of reaction for C=C and C=O bond hydrogenation of maleic anhydride on the Pd(1 1 1) surface. The hydrogenation of maleic anhydride to succinic anhydride is mildly exothermic with a surface energy of reaction of -14 kJ/mol. This is 133 kJ/mol less exothermic than the corresponding energy of reaction in the vapor phase. The Pd(1 1 1) surface hydrogenation of succinic anhydride to γ-butyrolactone, and γ-butyrolactone to THF, on the other hand, are endothermic by 32 and 63 kJ/mol, respectively. The analogous reactions in the vapor phase are highly exothermic with energies of reaction of -84 and -57 kJ/mol. The significant difference between the vapor phase and surface reaction energetics are due to the high dissociative adsorption energy of hydrogen on the Pd(1 1 1) surface.

In an effort to understand the detailed reaction mechanism, we have postulated an elementary reaction pathway for C–H bond formation in maleic anhydride hydrogenation. The hydrogenation of the C=C bond of maleic anhydride is postulated to proceed via the Horiuti–Polanyi mechanism, similar to that of ethylene. The transition state structure for this elementary reaction step was isolated by rigorous reaction-coordinate calculations of the reverse reaction of β-hydride elimination. The β-hydride elimination occurs via an agostic stretch of the C–H bond of the maleic anhydryl, followed by metal insertion into the C–H bond at the transition state. The activation barrier for the elementary reaction in maleic anhydride hydrogenation to maleic anhydryl, on a Pd_{19} cluster, is computed to be $+82$ kJ/mol and the energy of reaction is calculated to be -9 kJ/mol.

The ring opening reaction of maleic anhydride to form an oxametallacycle intermediate is also analyzed as a possible precursor to maleic anhydride decomposition on metals. The reaction coordinate for maleic anhydride ring opening, from the η^1 adsorption mode on Pd(1 1 1), was critically examined. Calculations indicate that the reaction has an activation barrier of $+163$ kJ/mol and is endothermic by 90 kJ/mol on Pd(1 1 1). The same reaction has a very low activation barrier of $+80$ kJ/mol and is exothermic by 96 kJ/mol on Re(0 0 0 1). Coupled with the fact that the η^1 adsorption energy of maleic anhydride on Re(0 0 0 1) is -172 kJ/mol, the ring opening reaction is non-activated on the Re(0 0 0 1) surface. This is consistent with the observations from UHV experiments [6].

Acknowledgements

We wish to thank the DuPont Chemical Company for their support of this work. Prof. Robert Davis (UVA), Prof. Brooks Pate (UVA) and Dr. Jan J. Lerou are also acknowledged for helpful discussions.

References

[1] C. Xu, W.D. Goodman, Langmuir 12 (1996) 1807–1816.
[2] M. Mabry, W. Prichard, S. Ziemecki, 1985, E.I. DuPont de Nemours and company, USP 4 550 185.
[3] M. Mabry, W. Prichard, S. Ziemecki, 1986, E.I. DuPont de Nemours and company, USP 4 609 636.
[4] M. Messori, A. Vaccari, J. Catal. 150 (1994) 177–185.
[5] M. Neurock, Stud. Surf. Sci. Catal. (1997).
[6] G. Coulston, DuPont CR&D, unpublished results.
[7] J. Andzelm, in: J. Labanowski, J. Andzelm (Eds.), Density Functional Methods in Chemistry, Springer, New York, 1991, pp. 155–169.
[8] J. Andzelm, E. Wimmer, J. Chem. Phys. 96(2) (1992) 1280–1303.
[9] Cray Research, Inc., Unichem Chemistry Codes, APG 5505, 1995.
[10] S.J. Vosko, L. Wilk, M. Nusair, Can. J. Phys. 58 (1980) 1200–1211.
[11] A.D. Becke, Phys. Rev. A 38 (1988) 3098.
[12] A. Becke, ACS Symp. Ser. 394 (1989) 165.
[13] J.P. Perdew, Phys. Rev. B 33 (1986) 8822.
[14] N. Godbout et al., Can. J. Chem. 70 (1992) 562.
[15] H. Chen, M. Krasowski, G. Fitzgerald, J. Chem. Phys. 98 (1993) 8710.
[16] N. Troullier, J.L. Martins, Phys. Rev. B 43 (1991) 1993.
[17] Cambridge Crystal Structure Database, Cambridge Crystallographic Data Centre, Cambridge, UK.
[18] P. Mirone, P. Chiorboli, Spectrochim. Acta 18 (1962) 1425–1432.
[19] C.J. Pouchert (Ed.), Aldrich Library of FT-IR Spectra, ed. I, vol. 3., Aldrich Chem. Co., Wisconsin, WI, 1989.
[20] J.E. DelBene (Ed.), Quantum chemical reaction enthalpies, Molecular Structure and Energetics, vol. 1, VCH, Weinhein, 1986.
[21] V. Pallassana, M. Neurock, Chem. Eng. Sci. (1999), ISCRE-15 Special issue.
[22] D.R. Lide (Ed.), CRC Handbook of Chemistry and Physics, 74th ed., CRC Press, Baca Raton, 1993–1994.
[23] P.A. Redhead, Vacuum 12 (1962) 203.
[24] V. Pallassana, M. Neurock, G. Coulston, 1999, J. Phys. Chem. B, submitted.
[25] H. Xu, C. Friend, J. Phys. Chem. (1992).
[26] H. Conrad, G. Ertl, E.E. Latta, Surf. Sci. 41 (1974) 435.
[27] W. Dong et al., Phys. Rev. B 54(3) (1996) 2157–2166.
[28] W. Dong, G. Kresse, J. Hafner, J. Mol. Catal. A 119 (1997) 69–76.
[29] J.F. Paul, P. Sautet, Phys. Rev. B 53(12) (1996) 8015.
[30] J.F. Paul, P. Sautet, Surf. Sci. 356 (1996) L403–L409.
[31] E.M. Stuve, S.W. Jorgensen, R.J. Madix, Surf. Sci. 146 (1984) 179–198.
[32] I. Horiuti, M. Polanyi, Trans. Faraday Soc. 30 (1934) 1164.
[33] V. Pallassana, M. Neurock, 1998, in preparation.